Molecular and Cellular Neuroscience 82 (2017) 204–217

Contents lists available at ScienceDirect

Molecular and Cellular Neuroscience

journal homepage: www.elsevier.com/locate/ymcne

Oxidative stress induced by cumene hydroperoxide produces synaptic depression and transient hyperexcitability in rat primary motor cortex neurons

R. Pardillo-Diaz [a,1], L. Carrascal [a,1], G. Barrionuevo [b], P. Nunez-Abades [a,*]

[a] Department of Physiology, School of Pharmacy, University of Seville, Spain
[b] Department of Neuroscience, University of Pittsburgh, Pittsburgh, PA, USA

ARTICLE INFO

Article history:
Received 13 March 2017
Revised 31 May 2017
Accepted 13 June 2017
Available online 15 June 2017

Keywords:
Lipid peroxidation
Pyramidal neurons
Cortical hyperexcitability
Postsynaptic currents
Amyotrophic Lateral Sclerosis

ABSTRACT

Pyramidal neurons of the motor cortex are selectively degenerated in Amyotrophic Lateral Sclerosis (ALS). The mechanisms underlying neuronal death in ALS are not well established. In the absence of useful biomarkers, the early increased neuronal excitability seems to be the unique characteristic of ALS. Lipid peroxidation caused by oxidative stress has been postulated as one of the possible mechanisms involved in degeneration motor cortex pyramidal neurons. This paper examines the effect of lipid peroxidation on layer V pyramidal neurons induced by cumene hydroperoxide (CH) in brain slices from wild type rats. CH induces a synaptic depression of pyramidal neurons in a time dependent manner, already observable on GABAergic synaptic transmission after 5 min application of the drug. Altogether, our whole-cell patch-clamp recording data suggest that the functional changes induced by CH upon pyramidal neurons are due to pre- and postsynaptic mechanisms. CH did not alter mEPSCs or mIPSCs, but decreased the frequency, amplitude, and decay rate of spontaneous EPSCs and IPSCs. These effects may be explained by a presynaptic mechanism causing a decrease in action potential-dependent neurotransmitter release. Additionally, CH induced a postsynaptic inward current that underlies a membrane depolarization. Depressing the input flow from the inhibitory premotor interneurons causes a transient hyperexcitability (higher resistance and lower rheobase) in pyramidal neurons of the motor cortex by presumably altering a tonic inhibitory current. These findings, which resemble relevant cortical pathophysiology of ALS, point to oxidative stress, presumably by lipid peroxidation, as an important contributor to the causes underlying this disease.

1. Introduction

Amyotrophic Lateral Sclerosis (ALS) is a fatal disease that results from degeneration of both the lower and upper motor neurons, including the motor cortex layer V of pyramidal neurons that regulate voluntary control of motor output (Mochizuki et al., 2011). Upper motor neuron degeneration causes spasticity, hyperreflexia and compromises motor control, while degeneration of lower motoneurons is characterized by muscular weakness and cell death (Boillée et al., 2006; Kim et al., 2014). In a small percentage of cases, the origin of the ALS has a genetic component, but 90% of cases are sporadic, and the initial cause is still unknown. Motoneuron degeneration in sporadic ALS may be the consequence of a combination of mechanisms, including excitotoxicity that triggers mitochondrial dysfunctions and deregulation of Ca^{2+} homeostasis, aberrant protein aggregation, neuroinflammation, altered ionic channels and excitability, and environmental toxicity (Cleveland and Rothstein, 2001; Foran and Trotti, 2009; Grosskreutz et al., 2007; Guatteo et al., 2007; Martorana et al., 2012; Philips and Robberecht, 2011; Pieri et al., 2013, 2009; Saba et al., 2016; Van Den Bosch et al., 2006; Yin et al., 2017; Zona et al., 2006). It is also widely believed that oxidative stress has a major role in the development of such a disease (Niedzielska et al., 2016; Poppe et al., 2014; Reynolds et al., 2007). In fact, a clinical study demonstrated that the magnitude of oxidative stress correlated well with clinical severity in patients with ALS (Ikawa et al., 2015). Furthermore, postmortem studies also reveal extensive damage of lipids, proteins, and DNA due to oxidative stress (Bogdanov et al., 2000). In addition, some of the above mentioned alterations may also be linked to an excessive activation of glutamate receptors that induce an excitotoxicity cascade (Spalloni et al., 2013). Studies with transcranial magnetic stimulation have demonstrated cortical hyperexcitability in patients with ALS, which were detected before the onset of symptoms of the disease (Vucic et al., 2011, 2008). From these findings, it has been proposed that motoneurons degeneration in ALS may be the result of cortical hyperexcitability, which would induce modifications of glutamatergic activity in cortical neurons.

* Corresponding author at: Facultad de Farmacia, Universidad de Sevilla, C/ Profesor García González n°2, 41012 Sevilla, Spain.
E-mail address: pnunez@us.es (P. Nunez-Abades).
[1] These authors contributed equally to this work.

http://dx.doi.org/10.1016/j.mcn.2017.06.002
1044-7431/

Therefore, increased release of glutamate from presynaptic terminals could induce excitotoxicity in upper and lower motoneurons (King et al., 2016; Maekawa et al., 2004). However, there is also evidence that cortical inhibition is disrupted in ALS (Geevasinga et al., 2014). Therefore, more accurate characterization is needed to determine whether there is an increase of excitation or a disruption of inhibition to explain the cortical hyperexcitability, and their contribution to motoneuron excitotoxicity in ALS.

We have previously demonstrated that 10 μM of CH evokes lipid peroxidation in a time dependent manner (Pardillo-Díaz et al., 2016). Lipid peroxidation caused by oxidative stress can be described generally as a process under which oxidants such as free radicals affect lipids containing carbon-carbon double bonds. Lipid peroxidation modifies membrane barrier properties increasing the permeability for water and ions, and to a lesser extent, high molecular weight compounds (Ferretti and Bacchetti, 2011; Nam, 2011). The organic oxidizing agent, cumene hydroperoxide (CH), has been used to inflict oxidative stress in in vivo studies (Muñoz et al., 2017). This agent penetrates the membrane lipid bilayer causing not only peroxidation of lipids, but also reacting with aminoacids, and proteins, as singlet oxygen does (reviewed in Ayala et al., 2014). In previous in vitro work from our laboratory, we have also demonstrated that oxidative stress, induced by CH, evokes dose and time dependent changes in the functional properties of pyramidal neurons from the motor cortex, compromising both neuronal excitability, and the capability of generating action potentials (Pardillo-Díaz et al., 2016, 2015). Specifically, resting membrane potential of pyramidal cells of the motor cortex under CH exposure become progressively depolarized with no changes in voltage threshold. Furthermore, membrane resistance shows a biphasic change on membrane resistance, increasing after 5 min of drug application and then it started to decrease, even under control values, after longer periods of exposure. At the same time, changes in membrane resistance produce compensatory variations in the rheobase that lead to a transient increase in excitability. In some neurons, long exposure to the drug caused loss of their ability to discharge repetitively action potentials. However, most of the neurons maintain their repetitive discharge even though their maximum frequency and gain decreased. Furthermore, cancelation of the repetitive firing discharge took place at intensities that decreased with larger drug concentration and/or longer time of exposure to CH, which resulted in a narrower working range. These changes are thought to be mainly caused by changes in the intrinsic membrane properties of the pyramidal cells (Pardillo-Díaz et al., 2016, 2015). However, in hypoglossal motoneurons, Nani and colleagues have shown that oxidative stress also affects synaptic transmission that is accompanied by a significant diminution in the frequency of spontaneous postsynaptic currents due to changes in the release of several neurotransmitters (Nani et al., 2010). Additionally, it also has been shown that hydrogen peroxide application decreases synaptic inhibition in cortical neurons (Frantseva et al., 1998). Therefore, we propose that some of the reported changes in membrane resistance and rheobase could be the result of modifications in the release of neurotransmitters on pyramidal neurons. As a consequence, further studies are needed to evaluate the influence of synaptic transmission on pyramidal cells from the motor cortex under CH exposure.

To that end, we obtained electrophysiological recordings from pyramidal motor cortex neurons in brain slices to examine the effects of lipid peroxidation on synaptic and membrane properties. Our study aims to address the following questions: i) Does oxidative stress affect synaptic transmission? ii) Are some synaptic inputs to pyramidal neurons more sensitive than others to the exposure to CH. iii) Is synaptic transmission recoverable after washout of the drug? iv) Are the reported changes in membrane resistance and rheobase due to the result of modification in the release of neurotransmitters on pyramidal neurons? v) Does alteration of inhibitory premotor synaptic inputs underlie the hyperexcitability of cortical neurons? The answers to these questions could be potentially relevant to understand the role of lipid peroxidation in some neurological diseases such as ALS.

2. Material and methods

2.1. Animals and slice preparations

All procedures were conducted in strict accordance with the recommendations of the *Guide for the Care and Use of Laboratory Animals of the European Community Directive 2003/65* and the *Spanish Royal Decree 120/2005*. The research protocol was approved by the Animal Ethics Committee of the University of Seville. Every effort was made to minimize the number of animals used and their suffering. Wistar rats (20–40 days of age) of both sexes were deeply anaesthetized with chloral hydrate (4%, Panreac) and decapitated. Brains were quickly removed and placed in ice-cold artificial cerebrospinal fluid (ACSF). This cutting solution was a low-calcium-ACSF. Transverse 300-μm-thick slices that included the primary motor cortex were cut on a vibratome (NVLSM1, WPI) kept at 35° for 30 min in an ACSF-filled chamber after slicing, and then stored at ~21 °C in the same solution until use. The composition of the ACSF (in mM) was as follows: 126 NaCl, 2 KCl, 1.25 NaH_2PO_4, 26 $NaHCO_3$, 10 glucose, 2 $MgCl_2$, and 2 $CaCl_2$. For the low-calcium-ACSF solution, the concentrations were 4 $MgCl_2$ mM and 0.1 $CaCl_2$ mM. Both ACSF and low-calcium-ACSF solutions were bubbled with 95% O_2-5% CO_2 (pH 7.4).

2.2. Whole-cell patch clamp recordings

Slices containing the primary motor cortex were transferred to a recording chamber and superfused at 1–2 ml·min^{-1} with recirculating aerated ACSF warmed to 33° ± 1 °C via a feedback-controlled heater (TC 324B; Warner). Neurons were whole cell patch voltage clamped under visual guidance using a Nikon Eclipse FN1 microscope equipped with infrared-differential interference contrast (IR-DIC) optics, a 40× water immersion objective, and a WAT-902H2 Ultimate Camera. Cortical pyramidal neurons were distinguished by their typical morphology including a rhomboidal cell body, a prominent apical dendrite extending vertically towards the surface and basal dendrites radiating out from the base of the soma (Fig. 1A–B). Patch pipettes were pulled (PC-10, Narishige) from borosilicate glass capillary with filament (inner diameter 0.6, outer diameter 1 mm; Narishige). For voltage-clamp experiments, patch electrodes had 3–4 MΩ resistance, whereas for current-clamp experiments they had 5–6 MΩ resistance. Patch pipettes were filled with intracellular solution containing (in mM): 125 MeSO4·Cs, 10 KCl, 10 HEPES, 0.5 EGTA, 2 ATP-Mg, 0.3 GTP-Na2 (pH 7.2 with CsOH; 285 ± 5 mOsm) for voltage-clamp experiments and MeSO4·Cs, that minimized the leak current of the recorded cell, was used to enable larger changes in voltage threshold. For current-clamp experiments, patch pipettes contained (in mM): 120 K-gluconate, 10 KCl, 10 phosphocreatine disodium salt, 2 MgATP, 0.3 NaGTP, 0.1 ethyleneglycol-bis (2-aminoethylether)-N,N,N′,N′-tetra acetic acid (EGTA), 10 4-(2-hydroxyethyl)-1-piperazineethanesulfonic acid (HEPES), adjusted to pH 7.3 with KOH. The osmolarity of intracellular solution was 285 mosmol/kg adjusted with sucrose. Whole-cell recording configuration was obtained using a micromanipulator (MP-225, Sutter) and a patch-clamp amplifier (Multiclamp 700B, Axon Instruments, Molecular Devices). Giga seals (>1 GΩ) were always obtained before rupture of the patch and pipette capacitance was compensated for before breaking in. In current-clamp mode, the bridge was periodically balanced using the auto-adjust feature. Throughout voltage-clamp recordings, the whole-cell capacitance and series resistance were measured and resistances were compensated by 70%. Recordings were discontinued if the series resistance increased by >50% or exceeded 20 MΩ.

2.3. Drugs and general protocol

All drugs were prepared just prior to experiments from stock solutions stored at −20 °C. The following drugs were used: 6-cyano-7-nitroquinoxaline-2,3-dione (CNQX, 50 μM), d-amino-phosphonovalerate

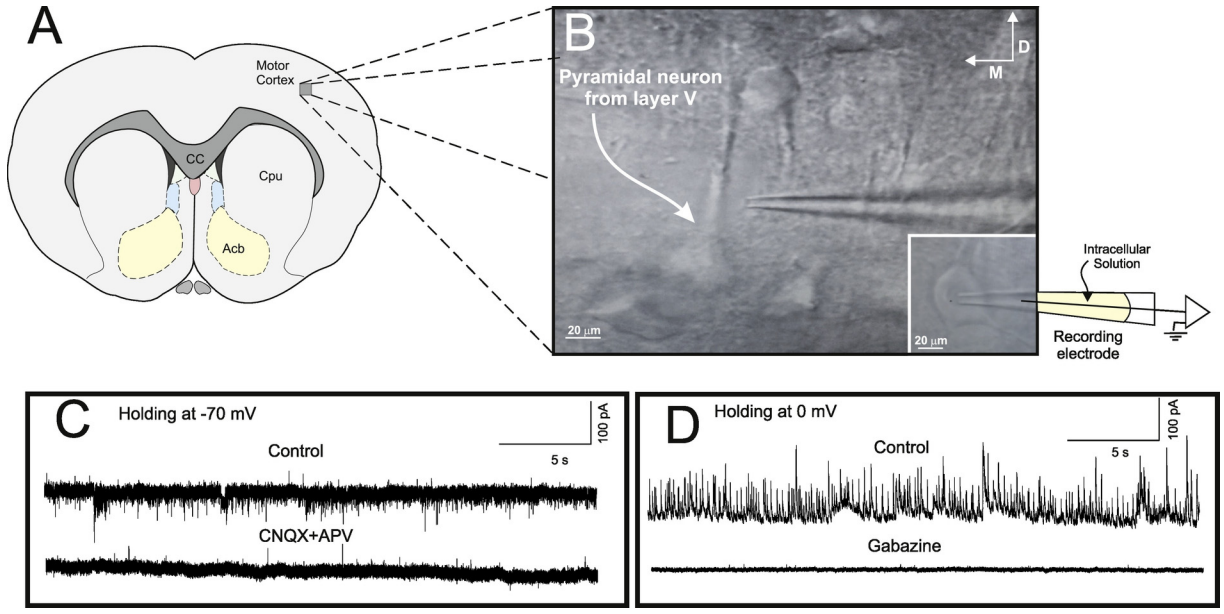

Fig. 1. Effects of CNQX, APV and Gabazine on spontaneous postsynaptic currents of pyramidal neurons from the motor cortex. (A) Drawing of a transverse section showing the location of the recorded area (primary motor cortex). Abbreviations: Acb, Acumbens nucleus; CPu, Caudate Putamen; CC, Corpus Callosum. (B) Typical neuron from the motor cortex patch clamped under direct visual control. (C) Effect of CNQX (50 μM) and AP-5 (25 μM) on spontaneous excitatory postsynaptic currents (sEPSC). (D) Effect of Gabazine (10 μM) on spontaneous inhibitory postsynaptic currents (sIPSC). Note that excitatory and inhibitory synaptic inputs are glutamatergic and GABAergic, respectively.

(APV, 20 μM), 2-(3-carboxypropyl)-3-amino-6-methoxyphenyl-pyridazinium bromide (SR95531 or gabazine, 20 μM) and tetrodotoxin (TTX, 1 μM) and purchased from Tocris (Bristol, UK). Cumene hidroperoxide was purchased from Sigma Aldrich and was applied at 10 μM concentration because we have demonstrated that this dose produce lipid peroxidation and electrophysiological changes of in vitro primary motor cortex neurons (Pardillo-Díaz et al., 2016, 2015).

In general, the protocol used for studying the effects of drugs was as follows: each neuron was initially superfused with normal ACSF to obtain voltage or current clamps recordings under control conditions. After this, to determine the effect of the different drugs, the slice was superfused with ACSF containing the drugs and current or voltage responses were again acquired. To avoid concerns associated with incomplete drug washout or incomplete recovery to control conditions, only one cortical neuron per slice was recorded.

2.4. Voltage clamp recordings and analysis

To know the effects of CH on inhibitory (IPSC) and excitatory (EPSC) synaptic currents, spontaneous and miniature IPSC and EPSC were recorded at holding membrane potentials of 0 (inhibitory) and −70 (excitatory) mV. Currents were low-pass filtered at 2 kHz and data were digitized at 5–20 kHz with a Digidata 1550 analog-to-digital converter and acquired using pCLAMP 10 software (Molecular Devices). Data were stored on a computer disk and analyzed offline using Stimfit 0.14 software (https://github.com/neurodroid/stimfit). Synaptic events were detected over 60 s of continuous recording and spontaneous and miniature postsynaptic currents were analyzed as is summarized: First, we created a preliminary template by fitting a function to a single event. Then, we used this preliminary template to extract some more exemplary events using a high detection threshold and we made a final template by fitting a function to the average of the exemplary events. Finally, we extracted all events with the final template using a low detection criterion. False positive events were manually removed, and the average of the remaining events was fitted with a biexponential function. The following parameters are measured: i) Amplitude or peak from base was the difference between baseline and the peak value; ii) Rise time (10–90%) refers to the time required for the signal to change from 10% to 90% of the peak value (measured from the baseline); iii) Decay refer to the maximal slope during the falling phase of the signal; iv) Frequency was measured as the number of event per second. On the other hand, the change in the holding current amplitude evoked by the application of CH or others drug was calculated as the difference with the baseline level (Torres-Torrelo et al., 2014) by using Clampfit 10.4 (Molecular Devices) software. Origin 8.0 software (Originlab Corporation, Northampton, MA, USA) was used to represent cumulative probability plots of synaptic events.

2.5. Current clamp recordings and analysis

To investigate the drug effects on intrinsic membrane properties, current clamp experiments were performed. Recordings were low-pass Bessel-filtered at 10 kHz; data were digitized at 20 kHz and analyzed offline using Clampfit 10.4 software (Molecular Devices). Input resistance was determined by passing positive and negative square current steps (500 ms, 1 Hz; with 50 pA increments) and calculated as the slope of the current-voltage plot; when there was evidence of an inward rectification, or sag, the voltage value used for this latter plot was the value achieved at the peak. Others parameters like tonic or maximum firing gain, rheobase or voltage threshold were routinely calculated (Carrascal et al., 2010; Torres-Torrelo et al., 2012). Origin 8.0 software (Originlab Corporation, Northampton, MA, USA) was used for linear regression and diagram representation.

2.6. Statistical analysis

Data were expressed as mean ± standard error of the mean; *n* refers to the number of neurons, as indicated. For statistical calculations, we used GraphPAD Prism 6.01 software (GraphPad Software Inc., La Jolla, USA). Data distribution was first processed with a normality test (Shapiro-Wilk Test). To determine if there were statistical differences between parameters in control vs. experimental in the same cell, an ANOVA with repeated measures was used to compare the means of the different group treatments. If there were significant differences, then we used the Bonferroni test to perform pairwise comparisons between groups. To analyze if there were statistical difference between postsynaptic currents from different groups of cells, one group treated with TTX and the other treated during 30 min with CH, we used

Student's *t*-test. Two groups of data were considered statistically different if $P \leq 0.05$. The correlation between variables was measured by Pearson's correlation coefficient (r). An asterisk in tables and figures indicates statistical differences between control and CH exposition while a cross indicates differences between two consecutives groups.

3. Results

The aim of this work is to quantify excitatory and inhibitory synaptic activity from layer V pyramidal cells of rat motor cortex (P21-P-40) using whole-cell patch-clamp recordings techniques (Fig. 1A–B). In these experiments, all spontaneous inward currents recorded at −70 mV were excitatory and were blocked by the application of the glutamatergic antagonists CNQX and APV in the perfusion bath (Fig. 1C). At 0 mV, all spontaneous outward currents were inhibitory which were abolished by the application of gabazine (Fig. 1D).

3.1. Application of CH induced depression of excitatory synaptic inputs onto pyramidal neurons from the motor cortex

To investigate if the spontaneous glutamatergic synaptic inputs are modified by lipid peroxidation induced by the application of 10 μM CH, we performed whole-cell voltage-clamp recordings with Cs-Methanesulfonate filled electrode and holding at a voltage membrane of −70 mV. Fig. 2A illustrates recordings of spontaneous excitatory postsynaptic currents (sEPSC) from a pyramidal neuron in control condition, and after 5, 15 and 30 min of CH application. These traces show a decrease in spontaneous excitatory synaptic frequency after CH administration whereas individual sEPSC displayed smaller amplitudes that were more evident at 15 and 30 min of CH application. For the whole population (n = 20), the mean frequency of sEPSC (Fig. 2C) remained unchanged at 5 min but significantly decreased by 33% from control (1.59 ± 0.11 Hz) after 15 min (1.23 ± 0.13 Hz) of CH application. Fig. 2B, which illustrates the average recordings of sEPSC, shows with more accuracy the changes in event amplitude and shape from the traces illustrated in Fig. 2A. A progressive diminution of amplitude is observed that reaches statistical significance at 15 min. Thus, amplitude event decreased from −37.8 ± 2.3 pA in control condition to −26.6 ± 1.6 pA after 15 min of CH administration (Fig. 2D). Fig. 2F and G represent probability plots of event amplitude for the same neuron illustrated in A-B. Fig. 2F shows that the greatest number of sEPSC were in the region of the −30 pA in the control condition, and in the region of −15 and −20 pA at 15 and 30 min of the CH application. This figure also shows that events larger than 40 pA disappeared at 15 and 30 min of the CH application. Fig. 2G illustrates that CH induced a leftward shift in the event probability of sEPSC amplitude when the data were plotted in cumulative normalized diagrams, more evident at 15 min, without affecting threshold. On the other hand, the amplitude A_{50} (values reached by the 50% of postsynaptic currents) was 27.8 pA in control condition, diminished to 23.6 pA at 5 min, and diminished again to 17.0 and 16.1 pA at 15 and 30 min, respectively, of CH administration. Finally, in parallel to the decrease in frequency and amplitude, the decay time constant of sEPSC (Fig. 2E) also decrease significantly from 4.86 ± 0.79 in control situation to 3.37 ± 0.40 after 15 min of CH. Finally, prolonged washout for 30 min did not reverse the observed effects in frequency, amplitude, and decay time constant of sEPSC (30 min, not shown, n = 5).

To understand how lipid peroxidation induces neuronal damage, and to determine the relative contribution of presynaptic mechanisms underlying decreased sEPSC frequency and kinetics of neurotransmitter release, TTX (1 μM) was added to observe action potential-independent release (Fig. 3A). This figure and Fig. 3C, show that event frequency of miniature excitatory postsynaptic currents (mEPSC) did not change by CH administration. Moreover, to study the event shape, average mEPSC were recorded from individual cells (n = 10). Typical waveforms of average mEPSC are illustrated in Fig. 3B. No differences were found in mEPSC amplitude (Fig. 3D), rise time (10–90%; Fig. 3E) or decay time constant (Fig. 3F) after 15 min of CH application. No changes were found in distribution of mEPSC plotted in Fig. 3G or in the cumulative normalized diagrams plotted in Fig. 3H after CH application. The amplitude A_{50} also remained unchanged after CH application, 14.4 pA in absence of CH and 13.5 pA under CH conditions. In fact, values of frequency, amplitude, and decay time constant obtained in mEPSC obtained in the presence of TTX (Fig. 3C–E) are similar to those obtained in sEPSC after 30 min of CH application (Fig. 2C–E). Since size and duration of sEPSC are determined by the amount of glutamate released, reducing glutamate release speed up the decay of the EPSC (Takahashi et al., 1995). Our data suggest that the fall of glutamate concentration in the synaptic cleft may explain the decay of the EPSC. From these data, we conclude that effects of CH in synaptic release can be explained by the blocking of the component of the sEPSC that is action potential mediated without affecting the mechanisms governing the fusion of vesicles with the membrane, glutamate uptake and properties of the postsynaptic glutamatergic receptors.

3.2. Application of CH induced depression of inhibitory synaptic inputs onto pyramidal neurons from the motor cortex

The CH-mediated synaptic depression evoked by CH at excitatory glutamatergic neurotransmission, may have also be extended to the release of inhibitory transmitters. To assess if the spontaneous GABAergic synaptic inputs were also modified by lipid peroxidation induced by the application of CH, we obtained whole-cell voltage-clamp recordings at a voltage membrane of 0 mV. Fig. 4A illustrates the recordings of spontaneous inhibitory postsynaptic currents (sIPSC) from a pyramidal neuron in control condition and after 5, 15 and 30 min of CH application. These traces show a drop in spontaneous synaptic events frequency after 5 min application of CH. The mean frequency of sIPSC (Fig. 4C) significantly decreased by 27% from control (6.96 ± 0.5 Hz) to 5 min of CH application (5.1 ± 0.34 Hz). Traces illustrating sIPSC average are shown in Fig. 4B. The average recordings show a progressive diminution of amplitude that reaches statistical significance respect to the control at 5 min of CH application. After 15 min of treatment, CH again produced a significant decrease in amplitude event; however, no significant difference was found between 15 min and 30 min of treatment. Thus, for the whole population (n = 20), amplitude event values decreased from 113.6 ± 11.5 pA in control condition to 75.10 ± 5.70 pA at 5 min of CH exposure, and then again decreased to 51.5 ± 3.4 (Fig. 4D) at 15 min of lipid peroxidation induction. Fig. 4F shows the probability plot of event amplitude for the example represented in Fig. 4A. This figure indicates that the majority of sIPSC had amplitudes around 35 pA in the control condition, and around 20 pA at 15 and 30 min after CH application. In this figure, it is also observable that events larger than 75 pA almost completely disappeared at 5 min of the CH application while in control condition a large number of events had amplitudes between 75 and 250 pA. Fig. 4G shows that CH induced a shift to the left in the event probability of sEPSC amplitude when the data were plotted in cumulative normalized diagrams, evident at 5 min of treatment. On the other hand, the amplitude A_{50} of sIPSC (values reached by the 50% of postsynaptic currents) was 107.6 pA in control condition, diminished to 39.2 pA at 5 min, and diminished again to 28.7 and 23.4 pA at 15 and 30 min, respectively, of CH administration. In parallel to the decrease in amplitude, the decay time constant of sIPSC (Fig. 4E) decreased progressively from 15.26 ± 0.6 ms in control situation to 13.85 ± 0.8 ms at 5 min and to 12.84 ± 0.7 after 15 min of CH application, reaching statistical significance. On the other hand, there was not washout of the observed effects in frequency, amplitude and decay time constant of sIPSC (not shown; n = 5).

We also recorded, in presence of TTX, miniature inhibitory postsynaptic currents (mIPSC, n = 10, Fig. 5A). This figure and Fig. 5C show that there is no change in mIPSC frequency after CH application. Fig. 5B illustrates typical waveforms of averaged mIPSCs from the example

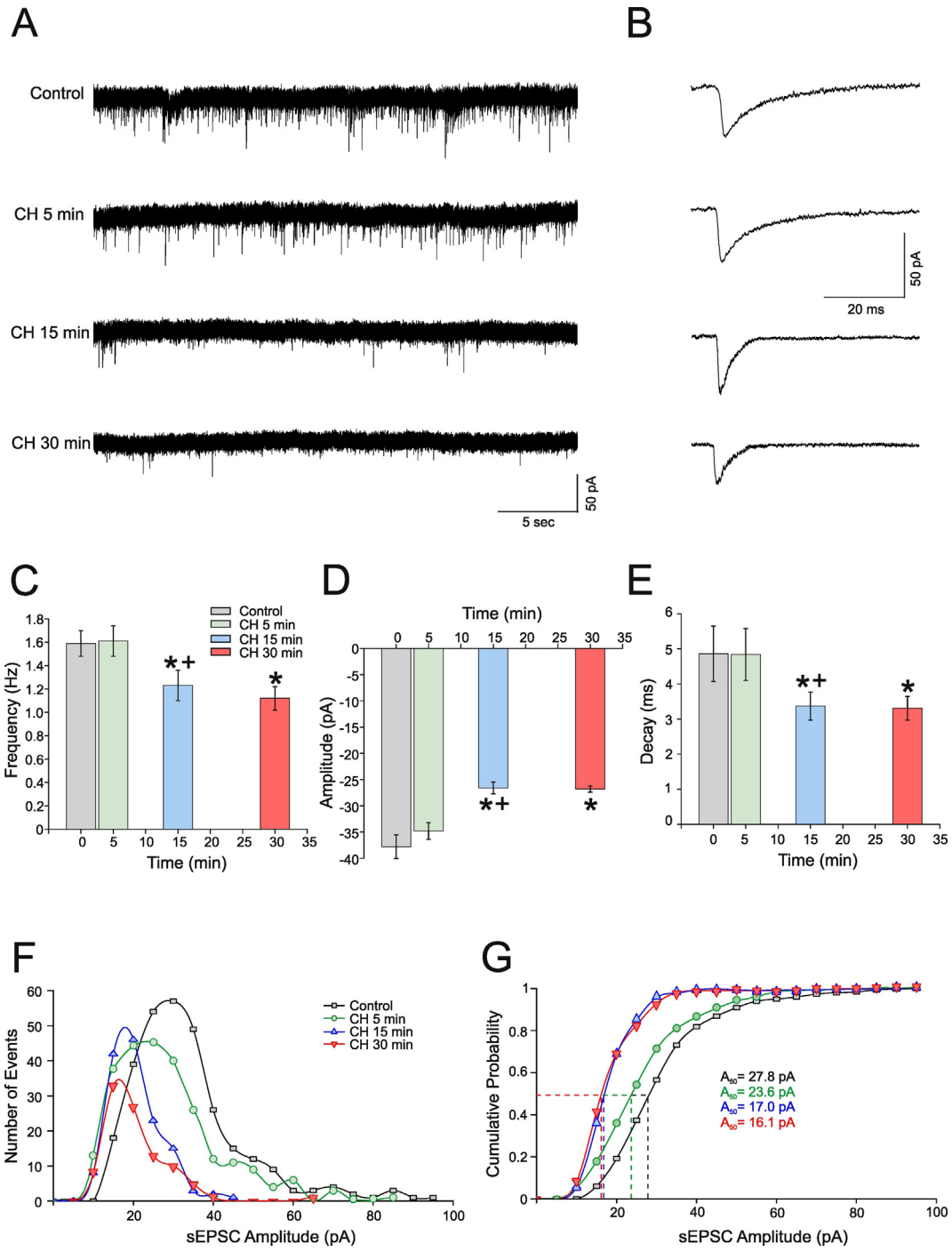

Fig. 2. Effects of cumene hydroperoxide (CH) on spontaneous excitatory postsynaptic currents (sEPSC) of pyramidal neurons from the motor cortex. (A) Whole-cell recordings of sEPSC in control conditions, and 5, 15 and 30 min after CH (10 μM) administration. (B) Traces illustrating sEPSC averages in control and after drug administration. (C–E) Histograms summarizing the mean values (n = 20) of frequency, amplitude, and decay in control conditions, and after CH administration. (F) Plot showing the relation between sEPSC number and amplitude for the four conditions. Note that CH induced a decrease in sEPSC frequency, and a shortening of sEPSC duration, as a consequence of a decrease in decay time constant after 15 min of CH application. (G) Cumulative normalized plots of sEPSC amplitude. The dashed lines show the amplitude (A_{50}) values reached by the 50% of sEPSC in each experimental situation. In all figures, the asterisk indicates statistical significance in relation to the control situation and a cross represents statistical significance between correlative measures.

represented in Fig. 5A showing that during 15 min of CH did not produce any change in event shape, amplitude (Fig. 5D), rise time (10–90%; Fig. 5E) or decay time constant (Fig. 5F). No differences were found in the distribution of mIPSCs plotted in Fig. 5G or the cumulative normalized diagrams plotted in Fig. 5H after CH application. The amplitude A_{50} remained unchanged from a value of 22–23 pA. These results suggest that mIPSCs are not affected by CH as previously found for the mEPSCs. Moreover, frequencies of mIPSCs are significantly lower to those obtained from ~~in~~ sIPSCs after 30 min of CH application. TTX reduce the frequency of IPSCs to 1.97 ± 0.27 Hz, while the frequency of IPSCs after 30 min of CH application was 3.93 ± 0.28. Furthermore, values of amplitude of mIPSCs obtained in the presence of TTX (27.1 ± 0.8 pA; Fig. 5D) were also smaller to those obtained in sIPSCs after 30 min of CH application (50.9 ± 3.8; Fig. 4D). We conclude from these data that inhibitory synaptic transmission is already disrupted after 5 min of CH exposure, but is not completely abolished after 30 min of CH.

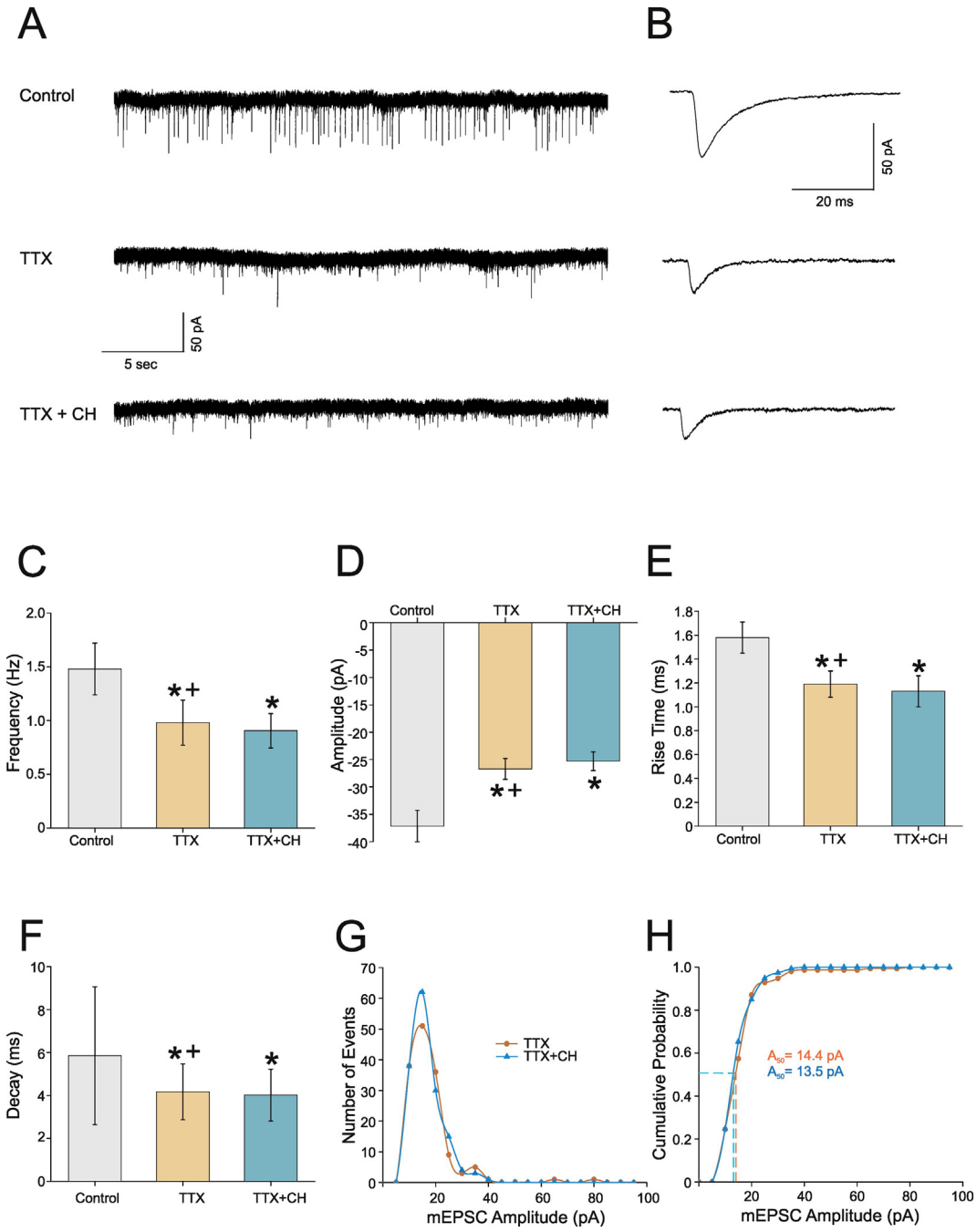

Fig. 3. Effects of cumene hydroperoxide (CH) on miniature excitatory postsynaptic currents (mEPSC) of pyramidal neurons from the motor cortex. (A) Whole-cell recordings showing excitatory postsynaptic currents (EPSC) in control conditions (spontaneous EPSC; sEPSC) (top), after tetrodotoxine (TTX; 1 μM) administration (mEPSC; middle) and the effect of 10 μM CH application during 15 min on mEPSC (bottom). (B) Traces illustrating EPSC averages in the three situations showed in A. (C—F) Histograms summarizing the mean values (n = 10) of frequency, amplitude, rise time (90–10%) and decay for all experimental conditions. (F) Plot showing the relation between mEPSC number in control condition and after CH application. (G) Cumulative normalized plots of mEPSC amplitude in control condition and after CH application. (G) Cumulative normalized plots of mIPSC amplitude in control condition and after CH application. The dashed lines show the amplitude (A_{50}) values reached by the 50% of mEPSC s in both situations.

3.3. Contribution of blockage of glutamatergic and GABAergic synaptic inputs in the effects of CH on neuronal excitability

Synaptic modifications produced by CH could have a direct action in the changes induced by this organic peroxide on neuronal intrinsic membrane properties and excitability. For a typical neuron, Fig. 6A depicted the effects of 10 μM CH administration on membrane potential during 20 min. The current-clamp recording shows a progressive depolarization that reaches its highest values (≈4 mV) at the end of the recording. To evaluate CH effects on input resistance, we used negative current steps (−100 pA, 200 ms) at 1 min intervals and voltage response were registered. CH produce a biphasic change on membrane resistance with a transient increase around 5 min after drug application, which then gradually declined under control values (Pardillo-Díaz et al., 2016, 2015). In Fig. 6A, neuron resistance increased from 182 MΩ in control to 203 MΩ 5 min after CH application. After this, it progressively decreased until reaching 150 MΩ at 15 min of recording. To explore any direct action of the action potential-dependent synaptic transmission in the biphasic change on membrane resistance, we eliminate premotor interneuron activity by applying TTX, and assessing the effects of CH on membrane input resistance and membrane potential. Fig. 6B illustrates that after 5 min of TTX administration an increase in the

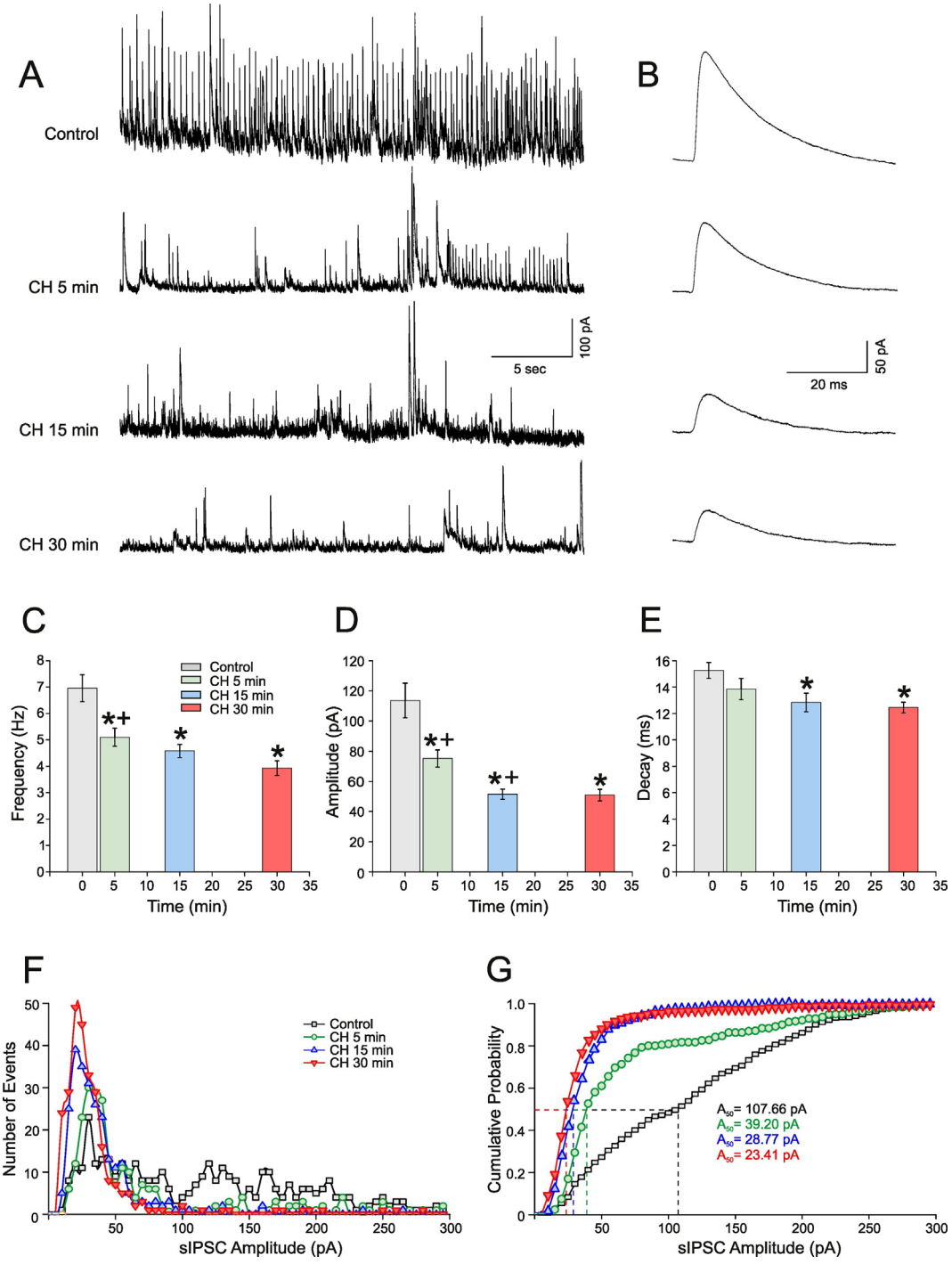

Fig. 4. Effects of cumene hydroperoxide (CH) on spontaneous inhibitory postsynaptic currents (sIPSC) of pyramidal neurons from the motor cortex. (A) Whole-cell recordings of sIPSC for control conditions, and 5, 15 and 30 min after CH administration (10 μM). (B) Traces illustrating sIPSC averages for control and after drug administration. (C–E) Histograms showing the mean values (n = 20) of frequency, amplitude and decay in control conditions, and after CH administration. (F) Plot showing the relation between sIPSC number and amplitude for the four conditions. Note that CH induced a decreased in sIPSC frequency and decay evident after 5 min of CH application. (G) Cumulative normalized plots of sIPSC amplitude. The dashed lines show the amplitude (A_{50}) values reached by the 50% of sIPSC s in each experimental situation.

amplitude of the voltage responses was observed, meaning that input resistance increased. Specifically, in this cell input resistance increase from control value of 146 MΩ to 162 MΩ. For the whole population (n = 12), input resistance was 142.4 ± 6.3 MΩ in control and significantly rose to 152.6 ± 5.3 MΩ in presence of TTX (Table 1). Moreover, as it can be noted in Fig. 6B, after 5 min of CH application, voltage response remained unchanged and no additional effect was observed in input resistance (Table 1). Afterward, it progressively diminished with time presenting values at 15 min of CH application below those of the control situation (Table 1), as is shown in Fig. 6B (129 MΩ). Regards to the effect on membrane potential, no effect of TTX was found, and a membrane potential depolarization of about 3 mV was detected after CH application (Fig. 6B; Table 1). From these data we conclude that the increase in membrane resistance typically observed during the first minutes of CH application may be synaptically mediated.

Fig. 6C illustrates the changes in holding current (Vh = −70 mV) during TTX followed by CH application. A slight inward current after TTX administration can be observed. In fact, for the whole population

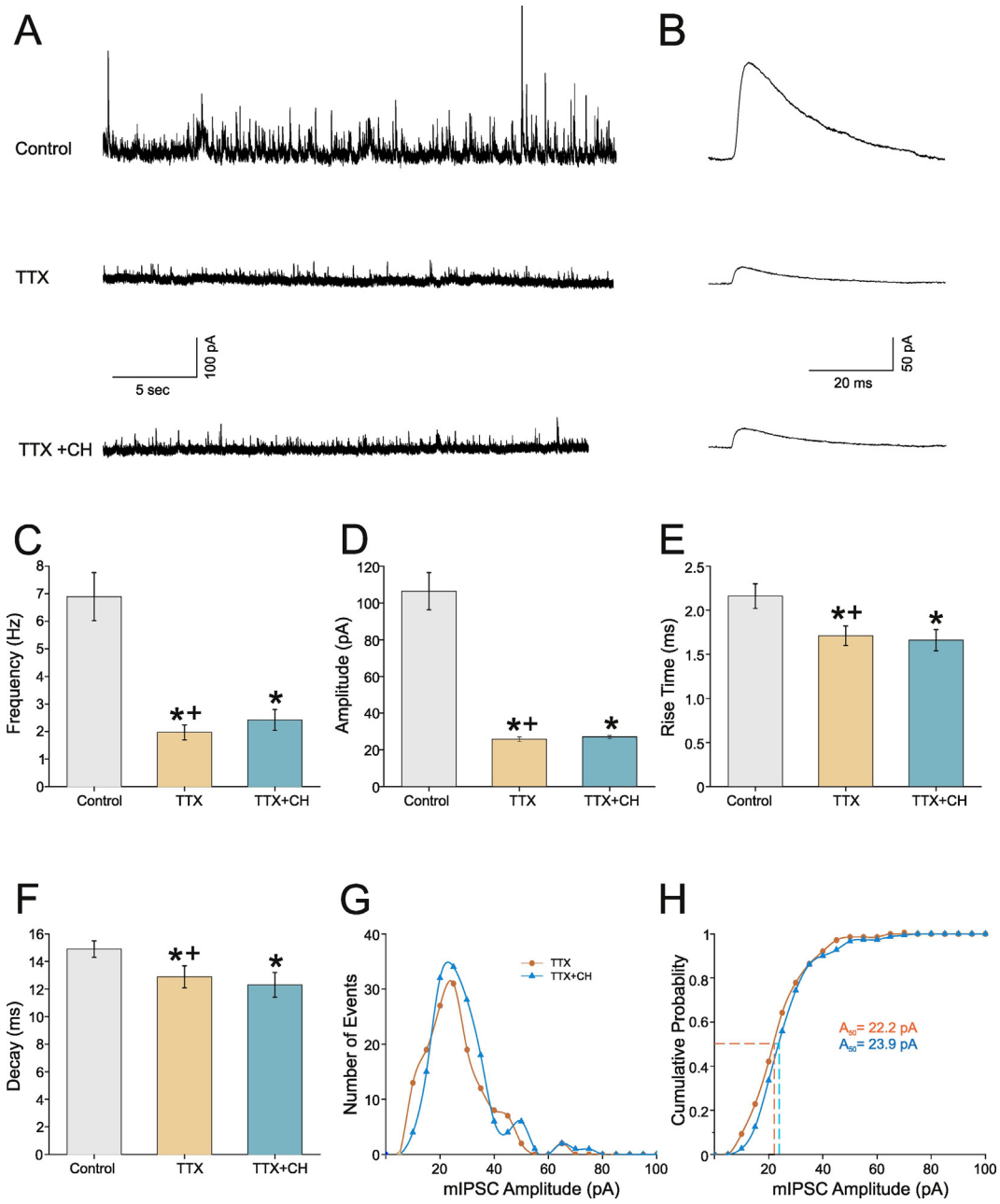

Fig. 5. Effects of cumene hydroperoxide (CH) on miniature inhibitory postsynaptic currents (mIPSC) of pyramidal neurons from the motor cortex. (A) Whole-cell recordings showing inhibitory postsynaptic currents (IPSC) in control conditions (spontaneous IPSC; sIPSC) (top), after tetrodotoxine (TTX; 1 μM) administration (mIPSC; middle) and the effect of 10 μM CH application during 15 min on mIPSC (bottom). (B) Traces illustrating IPSC averages in the three situations showed in A. (C–F) Histograms illustrating the mean values (n = 10) of frequency, amplitude, rise time (90–10%), and decay for all experimental situations. (F) Plot showing the relation between mIPSC number in control condition and after CH application. (G) Cumulative normalized plots of mIPSC amplitude in control condition and after CH application. (G) Cumulative normalized plots of mIPSC amplitude in control and after CH application. The dashed lines show the amplitude (A_{50}) values reached by the 50% of mIPSC in both situations.

of cells (n = 12) the inward current observable after TTX application was −10.0 ± 4.4 pA (Table 1). Application of CH elicited a slow and significant increase in holding current that was, for the whole population, −17.9 ± 6.4 pA after 5 min and −42.5 ± 13.8 pA after 15 min (−44 pA for the neuron illustrates in Fig. 6C) of CH application. These data suggest that CH caused an inward (depolarizing) current, through a mechanism that is, at least, in part insensitive to TTX, and not blocked by intracellular Cs^+ included in the path microelectrode. We conclude that this inward current may underlie the depolarization we observed in pyramidal neurons under CH exposure.

To examine the contribution of glutamatergic and GABAergic synaptic inputs to the effects of TTX and CH in membrane properties we carried out experiments with neurotransmitter antagonists. Blockade of phasic excitatory transmission with CNQX and APV did not prevent the effects by CH on membrane depolarization or the observed biphasic change on input resistance (see Table 2). Blockade of inhibitory synaptic transmission with gabazine ($GABA_A$ blocker) eliminate the effects by CH that produces the transient increase on membrane resistance about 5 min of exposure to the drug. Fig. 7A–D illustrates the recordings from a typical cell showing membrane potential responses to negative and positive current steps of 50 pA in control conditions, after gabazine addition, and after application of a mixture of gabazine and CH. As seen in Fig. 7E, input resistance of this neuron shifted from 181 to 208 MΩ after blockade of GABAergic receptors with gabazine. Input resistance remained unchanged, 205 MΩ after 5 min of CH application, and later diminished to 119 MΩ after 15 min administration. These results are

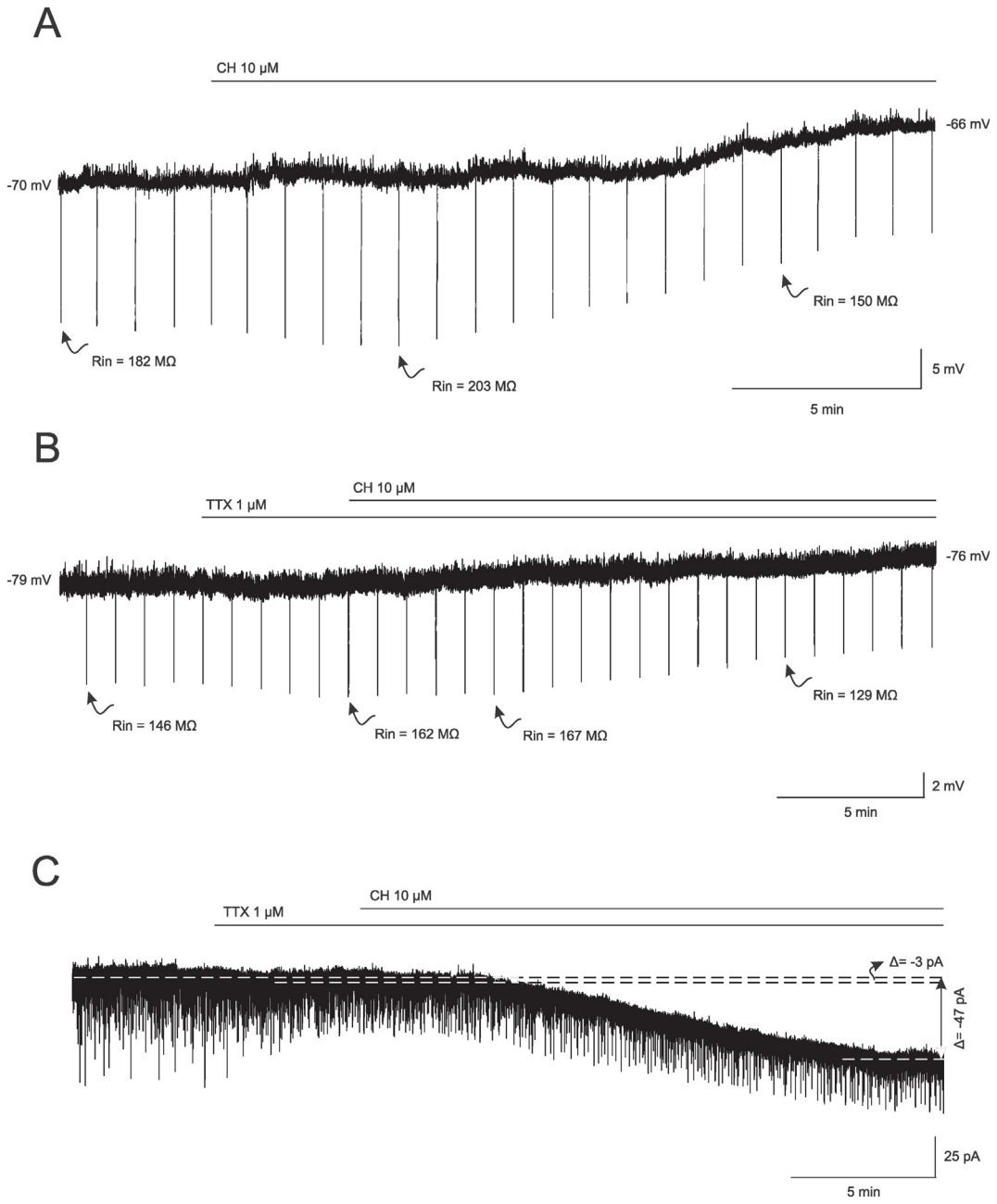

Fig. 6. Effects of tetrotodotoxin (TTX) and cumene hydroperoxide (CH) on input resistance (Rin), membrane potential and holding current of pyramidal neurons from the motor cortex. (A) Current clamp recording showing the typical voltage response to negative current pulses (−100 pA) in control condition (first arrow from the left) and during the administration of 10 μM CH (5 min, second arrow; 15 min, third arrow). Note a transient increase in the amplitude of the voltage responses after CH application (increase resistance) followed by a membrane potential depolarization and a final decrease in input resistance. (B) Voltage response to negative current pulses (−100 pA) in control condition (first arrow from the left), after 5 min of TTX (1 μM) administration (second arrow) and after CH treatment (5 min, third arrow; 15 min, fourth arrow). Note an increase in the amplitude of the voltage responses after TTX application (increase resistance) that remained unchanged after the first 5 min of CH application. Later, it progressively diminished after recording for 15 more minutes. Also a membrane potential depolarization was observed. (C) Voltage clamp recording showing the time course of changes in holding current (Vh = −70 mV) after TTX and CH administration. Note that TTX and CH administration caused inward currents of −3 pA and −44 pA, respectively.

similar from all recorded cells (n = 12; Table 3). Input resistance significantly increases after gabazine application respect to control while remained unchanged after 5 min of CH. Later, after 15 min of CH

Table 1
Effects of tetratodotoxin (TTX) and cumene hydroperoxide (CH) on resting membrane potential (RMP), input resistance (Rin) and holding current of pyramidal neurons from the motor cortex.

n = 12	Control	TTX	CH 5 min	CH 15 min
RMP (mV)	−70.3 ± 0.8	−70.7 ± 0.7	−68.2 ± 1.0*+	−67.0 ± 1.0*
Rin (MΩ)	142.4 ± 6.3	152.6 ± 5.3*+	157.8 ± 4.6*	121.8 ± 4.4*+
Baseline (pA)		−10.0 ± 4.4*+	−17.9 ± 6.4*+	−42.5 ± 13.8*+

Table 2
Effects of CNQX and APV on resting membrane potential (RMP) and input resistance (Rin) of pyramidal neurons from the motor cortex.

n = 12	Control	CNQX + APV	CH 5 min	CH 15 min
RMP (mV)	−74.5 ± 1.1	−72.9 ± 1.2	−69.9 ± 1.5*+	−67.0 ± 1.6*+
Rin (MΩ)	142.7 ± 8.7	145.0 ± 8.2	160.7 ± 8.1*+	127.5 ± 8.2*+

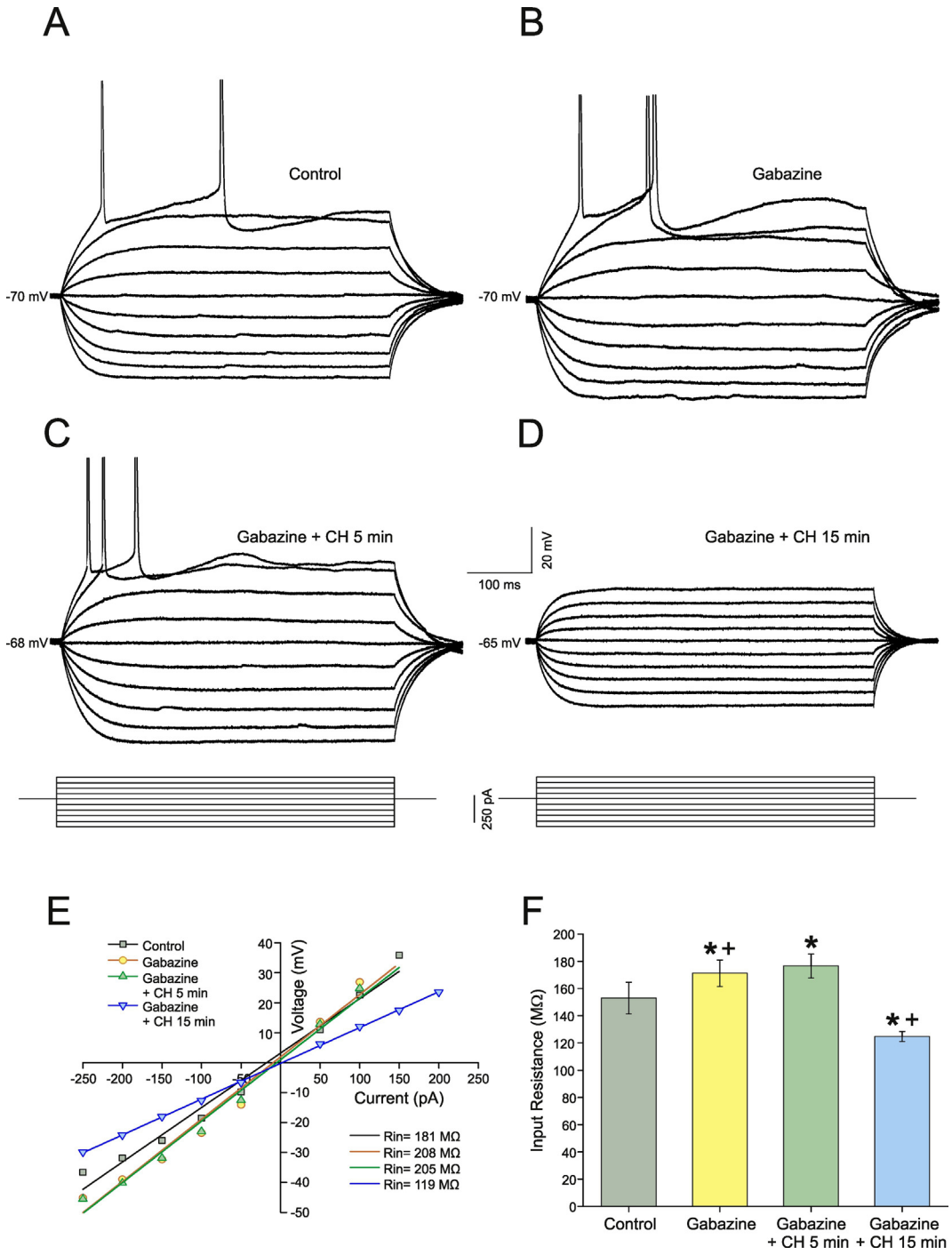

Fig. 7. Effects of Gabazine and cumene hydroperoxide (CH) on input resistance of pyramidal neurons from the motor cortex. (A–D) Recordings from the same cell showing membrane potential responses to negative and positive current steps of 50 pA in control conditions (A), after Gabazine addition (10 μM) (B), and 5 and 15 more minutes of Gabazine plus 10 μM CH administration (C and D). Action potentials have been truncated in these figures. (E) Plot illustrating the relation between current and voltage response for the cell represented in A–D. Note that Gabazine produced an increase in input resistance. (F) Histogram summarizing the mean values of input resistance in control conditions and the other three situations for the whole population (n = 12).

Table 3
Effects of Gabazine on resting membrane potential (RMP) and input resistance (Rin) of pyramidal neurons from the motor cortex.

n = 12	Control	Gabazine	CH 5 min	CH 15 min
RMP (mV)	−75.8 ± 1.4	−74.8 ± 1.1	−70.6 ± 1.5*+	−69.7 ± 1.7*
Rin (MΩ)	153.0 ± 8.2	171.2 ± 9.7*+	176.6 ± 9.8*	124.8 ± 2.6*+

application, input resistance decreases reaching values smaller to those measured in control situation (Fig. 7F). A functional consequence of the increase in resistance in the presence of gabazine and 5 min of exposure to CH is that the pyramidal cell in Fig. 7 shows a decrease in rheobase as compared to control condition. In this cell, 100 pA evoked an action potential only with gabazine, and after 5 min of gabazine plus CH application. From these data, we conclude that blocking GABAergic inputs with gabazine produces similar results to those observed with the application of TTX. Furthermore, the transient increase in membrane resistance after 5 min of CH application may be due to the block of a tonic

inhibitory current, mediated by GABA, as a consequence of presynaptic depression of SIPCs. Blocking these inhibitory synaptic inputs on pyramidal cells, which we demonstrated is already present after 5 min of exposure to CH, may undergo a transient phase of hyperexcitability as a consequence of the lipid peroxidation.

4. Discussion

Cortical hyperexcitability is an early feature of ALS. The main finding of the present study is that lipid peroxidation induced by CH produce significant alterations of synaptic inputs to layer V motor cortex pyramidal neurons. Thus, CH induced a time-dependent synaptic depression on pyramidal neurons being GABAergic transmission the first input affected. This latter finding triggered a transient pyramidal hyperexcitability characterized by an increase in membrane resistance (and then a decrease in rheobase), that could be due to the blocking of a tonic inhibitory current. In parallel CH evoked a depolarizing inward current. Our data suggest that functional changes induced by CH may be potentially relevant to explain the role that lipid peroxidation may have in ALS.

4.1. CH depress the input flow from the premotor interneurons

We demonstrated in previous in vitro works from our laboratory, that oxidative stress, induced by CH, evokes dose and time dependent changes in the functional properties of pyramidal neurons from the motor cortex, compromising both cell excitability, and the capability of repetitively discharge of action potentials (Pardillo-Díaz et al., 2016, 2015). We wonder whether some of the reported changes in membrane properties, in particular membrane resistance and rheobase, could be the result of modifications in the release of neurotransmitters on pyramidal neurons. It has been previously reported that oxidative stress induced by hydrogen peroxide, affects synaptic transmission on hypoglossal motoneurons causing a significant reduction in the frequency of spontaneous synaptic events (Nani et al., 2010). To evaluate the influence of synaptic transmission on pyramidal cells from the motor cortex, we have thoroughly looked at sEPSC and sIPSC analyzed in control condition, and after CH application to the bath. We selected a 10 μM CH concentration for 30 min, values that guarantee a death rate lower than 5% (Pardillo-Díaz et al., 2016; Vimard et al., 2011). Our results indicate that CH induces a synaptic depression of pyramidal neurons in a time dependent manner. Mean frequency of sEPSC remained unchanged at 5 min but significantly decreased by 33% from control after 15 min of CH application. Moreover, the mean frequency of sIPSC significantly decreased earlier by 27% from control to 5 min of CH application. These results are in agreement with a previous study reporting that hydrogen peroxide application for 4 min decreased IPSP by 35% of control in cortical and 42% in thalamic neurons, and after 6 min abolished inhibitory postsynaptic responses in 70% of cortical and in 67% of thalamic neurons (Frantseva et al., 1998). These authors also reported that the progressive decrease of inhibitory synaptic transmission starts almost immediately after hydrogen peroxide exposure.

Our results also indicate that amplitude and decay of sEPSC and sIPSC decrease by CH exposure. It is well known that the size and duration of sPSC are determined by the amount of neurotransmitter released because reducing neurotransmitter release speed the decay of the sPSC (Takahashi et al., 1995). Our data suggest that the fall of glutamate and GABA concentration, respectively, in the synaptic cleft may explain the decrease in amplitude and decay of the sPSC. Furthermore, in the presence of TTX to observe action potential-independent release, values of frequency, amplitude, and decay time constant obtained in mEPSC and mIPSC did not change after 15 min of CH application. From these data, we conclude that the effects of CH on synaptic amplitude and kinetics can be explained by the blocking of the component of the sPSC that are action potential mediated without affecting the mechanisms governing the fusion of vesicles with the presynaptic membrane, the rate of neurotransmitter uptake, and the properties of the postsynaptic neurotransmitter receptors. Previously, we have reported that long exposure to CH caused, in some neurons, a loss of their ability to discharge repetitively action potentials whereas in neurons that maintain repetitive discharge, gain and maximum frequency decreased (Pardillo-Díaz et al., 2016, 2015). From our findings, we conclude that the input flow from premotor interneurons to pyramidal neurons is extremely vulnerable to CH exposure. We have also demonstrated that exposure of brain slices to 10 μM of CH evokes lipid peroxidation in a time dependent manner. Longer time caused a progressive increase in lipid peroxidation, significant after 5 min in respect to the control. Furthermore, it was also observable lipid peroxidation with CH 1 μM (Pardillo-Díaz et al., 2016). We propose that observed effects of CH on synaptic transmission are due to lipid peroxidation. However, early studies showed that CH at concentrations below that required to alter lipid peroxidation induces Ca^{2+} release from mitochondria (Gogvadze and Zhukova, 1991; Bindoli, 1988). Then, we cannot discard that other mechanisms that trigger mitochondrial dysfunctions and deregulation of Ca^{2+} homeostasis may also be involved.

4.2. CH causes a depolarization that is synaptic independent

CH decreased the resting membrane potential of pyramidal neurons. The depolarization of the resting membrane may arise from an increase in an inward current and/or a decrease in an outward current. We have demonstrated that CH evoked a slowly developing inward current (depolarization) that is not mediated by neurotransmitter since it is observable in the presence of TTX. Nakaya and colleagues reported that in isolated guinea-pig cardiac cells, the membrane depolarization caused by CH was not associated with a decrease in potassium equilibrium potential resulting from leak of intracellular K^+ (Nakaya et al., 1992). These authors concluded that the depolarization of the resting membrane potential induced by oxidative stress was, at least in part, due to the inhibition of the inward rectifier K^+ channel activity. In leech neurons, application of hydrogen peroxide also produced changes in the electrical properties, including a membrane depolarization and inhibition of the outward potassium current responsible for the repolarization of action potentials (Jovanovic et al., 2016). Furthermore, Nani et al. (2010) found an inward current or membrane depolarization accompanied by an increase in input resistance evoked by hydrogen peroxide in hypoglossal motoneurons. This latter finding implied a depression of a leak background K^+ current that was not inhibited by intracellular Cs^+ contained in the patch pipette that could be responsible for the inhibition of TASK-1-type leak K^+ channels (Fisher and Nistri, 1993; Nani et al., 2010). Therefore, it could be proposed that the same currents may underlie the observed depolarization on pyramidal neurons after CH exposure. Regardless of which conductances and/or channels underlie changes in membrane potential and membrane resistance, we demonstrate that depolarization of the membrane potential and increase in membrane resistance under oxidative stress are not linked.

4.3. CH induced a transient increase in membrane resistance probably influencing a tonic inhibitory current

There is evidence that cortical inhibition is impaired in ALS (Zanette et al., 2002; Ziemann et al., 1997). Disruption in human cortical interneurons have been observed in studies of primary motor cortex, where calbindin-, parvalbumin- and neuropeptide Y positive interneurons may be lost in layer V and VI (Maekawa et al., 2004; Nihei and Kowall, 1993). In the wobbler mice, a model of ALS, it was found a decrease in the number of parvalbumin- and somatostatin-positive inhibitory interneurons and a decrement in the density of GABAergic synaptic boutons in the region of the motor cortex (Nieto-Gonzalez et al., 2011). Furthermore, in layer V pyramidal neurons of motor cortex, the frequency of $GABA_A$ receptor-mediated sIPSC was reduced by 72% and tonic inhibition mediated by extrasynaptic $GABA_A$ receptors was

also reduced by 87% when compared with wildtype mice (Nieto-Gonzalez et al., 2011). These authors concluded that pyramidal neurons of the wobbler mice display an increased input resistance and excitability by lack of $GABA_A$ receptor-mediated influences. Therefore, reduced GABAergic inhibition, might explain not only the cortical hyperexcitability in wobbler mice but also how pyramidal neurons exhibited an increase in resistance under oxidative stress after CH exposure.

It is expected that larger input resistance of motoneurons contribute to their higher excitability. Our data suggest that CH induce a synaptic depression that is already observable on GABAergic synaptic transmission after 5 min application of the drug. This latter observation correlates with the transient increase in input resistance, found in current clamp experiments, after 5 min of CH application. Our results suggest that the overall effect of lipid peroxidation induced by CH was to depress the input flow from the premotor interneurons that promote an unexpected transient hyperexcitability onto pyramidal neurons of the motor cortex. Hyperexcitable events in pyramidal neurons also were observed after hydrogen peroxide exposure (Frantseva et al., 1998). These authors concluded that oxidative stress contributes to the development of seizures in thalamocortical circuitry by attenuation of inhibitory neurotransmission, among other factors. It is known that GABAergic interneurons play a major role reducing neuronal excitability in the cortex (Wagle-Shukla et al., 2009) and other motoneuronal pools (Torres-Torrelo et al., 2014). GABAergic interneurons are involved in local circuit neurons that constitute approximately 15–20% of all neurons in the cortex, which during development adapt their function to enable fine motor movements (Batista-Brito and Fishell, 2009; Biane et al., 2015). It has been demonstrated that a tonic current activated by low GABA concentrations, that it can be blocked by gabazine, dominate GABAergic transmission in newborn neocortical pyramidal cells, exerting heterogeneous effects on neuronal excitability (Sebe et al., 2010). We propose that lipid peroxidation can elicit pyramidal neurons hyperexcitable thorough a combination of depression of GABAergic synaptic inputs that enhanced input resistance (that trigger a compensatory change of equal magnitude in rheobase) by altering a tonic inhibitory current.

4.4. Functional consequences of hyperexcitability

Cortical hyperexcitability is a common and early feature of ALS (Bae et al., 2013; Do-Ha et al., 2017; Vucic et al., 2008). In the absence of useful biomarkers identified from analysis of the blood and cerebrospinal fluid, the increased early cortical excitability distinguishes ALS from mimic disorders (Turner et al., 2009; Vucic et al., 2011). The glutamate excitotoxicity theory of ALS emphasize the contribution of excessive synaptic excitation, in part through glutamate receptors and Na^+ channels (Bogaert et al., 2010; Fogarty et al., 2016; Heath and Shaw, 2002; Kuo et al., 2005; Kwak et al., 2010; Sasabe and Aiso, 2010; Spalloni et al., 2013; Zona et al., 2006). An increased glutamate concentration was found in motor cortex of patients with ALS, as shown by 1H-magnetic resonance spectroscopy (Han and Ma, 2010; Pioro et al., 1999). However, the excitotoxicity theory is challenged by the inability of anti-glutamatergic agents to have major beneficial effect on ALS patients (Zoccolella et al., 2009). On the other hand, a new hypothesis is that pathogenic loss of local inhibitory circuitry might be related to the high level of functional connectivity in ALS (Martin and Chang, 2012; Turner and Kiernan, 2012). This latter hypothesis is further supported by decreased GABA concentrations in the primary motor cortex of patients with ALS, as demonstrated by 1H-magnetic resonance spectroscopy (Foerster et al., 2012) and PET marker of benzodiazepine receptor unit distribution in pyramidal cells (Lloyd et al., 2000). Abnormal GABA and glycine levels are observed in ALS patients (Malessa et al., 1991; Niebroj-Dobosz and Janik, 1999). In human ALS autopsy motor cortex, some $GABA_A$ receptor subunits show reduced levels of mRNA expression (Petri et al., 2003). Models of ALS give evidence for imbalanced excitatory and inhibitory innervations (Avossa et al., 2006; Fogarty et al., 2016). Zhang and colleagues used a TDP-43 A315T mouse model to demonstrate that impairments in GABAergic signaling contribute to cortical hyperexcitability (Zhang et al., 2016). Based in these findings, disrupted inhibition could have a role in ALS (Martin and Chang, 2012). A question arise from our results, is why inhibitory neurons are more sensitive to oxidative stress. Mutant Sod1 zebrafish model revealed that interneurons are the first neuronal population displaying stress, and that the reduction of inhibitory currents preceded any defects in motor neurons (McGown et al., 2013). Our patch-clamp data demonstrated that pyramidal neurons of the rat motor cortex receive a decreased inhibitory neurotransmission at the early stages of lipid peroxidation, without compensatory decrease in excitatory neurotransmission which enhanced input resistance and causing a transient hyperexcitability. Since cortical hyperexcitability seems to be an early characteristic in ALS, assuming that oxidative stress is a contributor to this pathology (Geevasinga et al., 2014; Vucic et al., 2011), we propose that lipid peroxidation may contribute to the causes behind neurodegenerative diseases such as ALS.

Acknowledgement

This work was partially supported by ERDF (European Regional Development Fund) UNSE10-1E-0949. Mr. Ricardo Pardillo-Diaz obtained a research fellowship funded by CACOF. We sincerely thank The Centre of Research Technology and Innovation of the University of Seville (CITIUS) for their technical support, and Ms. María Eugenía Martín-Pachón for her technical assistance.

References

Avossa, D., Grandolfo, M., Mazzarol, F., Zatta, M., Ballerini, L., 2006. Early signs of motoneuron vulnerability in a disease model system: characterization of transverse slice cultures of spinal cord isolated from embryonic ALS mice. Neuroscience 138: 1179–1194. http://dx.doi.org/10.1016/j.neuroscience.2005.12.009.

Ayala, A., Muñoz, M.F., Argüelles, S., 2014. Lipid peroxidation: production, metabolism, and signaling mechanisms of malondialdehyde and 4-hydroxy-2-nonenal. Oxidative Med. Cell. Longev. 2014:1–31. http://dx.doi.org/10.1155/2014/360438.

Bae, J.S., Simon, N.G., Menon, P., Vucic, S., Kiernan, M.C., 2013. The puzzling case of hyperexcitability in amyotrophic lateral sclerosis. J. Clin. Neurol. 9:65. http://dx.doi.org/10.3988/jcn.2013.9.2.65.

Batista-Brito, R., Fishell, G., 2009. Chapter 3 the developmental integration of cortical interneurons into a functional network. Current Topics in Developmental Biology: pp. 81–118. http://dx.doi.org/10.1016/S0070-2153(09)01203-4.

Biane, J.S., Scanziani, M., Tuszynski, M.H., Conner, J.M., 2015. Motor cortex maturation is associated with reductions in recurrent connectivity among functional subpopulations and increases in intrinsic excitability. J. Neurosci. 35:4719–4728. http://dx.doi.org/10.1523/JNEUROSCI.2792-14.2015.

Bindoli, A., 1988. Lipid peroxidation in mitochondria. Free Radic. Biol. Med. 5 (4), 247–261.

Bogaert, E., d'Ydewalle, C., Van Den Bosch, L., 2010. Amyotrophic lateral sclerosis and excitotoxicity: from pathological mechanism to therapeutic target. CNS Neurol. Disord. Drug Targets 9, 297–304.

Bogdanov, M., Brown, R.H., Matson, W., Smart, R., Hayden, D., O'Donnell, H., Flint Beal, M., Cudkowicz, M., 2000. Increased oxidative damage to DNA in ALS patients. Free Radic. Biol. Med. 29, 652–658.

Boillée, S., Yamanaka, K., Lobsiger, C.S., Copeland, N.G., Jenkins, N.A., Kassiotis, G., Kollias, G., Cleveland, D.W., 2006. Onset and progression in inherited ALS determined by motor neurons and microglia. Science 312:1389–1392. http://dx.doi.org/10.1126/science.1123511.

Carrascal, L., Luque, M.A., Sobrino, V., Torres, B., Nunez-Abades, P., 2010. Postnatal development enhances the effects of cholinergic inputs on recruitment threshold and firing rate of rat oculomotor nucleus motoneurons. Neuroscience 171:613–621. http://dx.doi.org/10.1016/j.neuroscience.2010.09.001.

Cleveland, D.W., Rothstein, J.D., 2001. From Charcot to Lou Gehrig: deciphering selective motor neuron death in ALS. Nat. Rev. Neurosci. 2:806–819. http://dx.doi.org/10.1038/35097565.

Do-Ha, D., Buskila, Y., Ooi, L., 2017. Impairments in motor neurons, interneurons and astrocytes contribute to hyperexcitability in ALS: underlying mechanisms and paths to therapy. Mol. Neurobiol. http://dx.doi.org/10.1007/s12035-017-0392-y.

Ferretti, G., Bacchetti, T., 2011. Peroxidation of lipoproteins in multiple sclerosis. J. Neurol. Sci. 311:92–97. http://dx.doi.org/10.1016/j.jns.2011.09.004.

Fisher, N.D., Nistri, A., 1993. Substance P and TRH share a common effector pathway in rat spinal motoneurones: an in vitro electrophysiological investigation. Neurosci. Lett. 153, 115–119.

Foerster, B.R., Callaghan, B.C., Petrou, M., Edden, R.A.E., Chenevert, T.L., Feldman, E.L., 2012. Decreased motor cortex γ-aminobutyric acid in amyotrophic lateral sclerosis. Neurology 78:1596–1600. http://dx.doi.org/10.1212/WNL.0b013e3182563b57.

Fogarty, M.J., Klenowski, P.M., Lee, J.D., Drieberg-Thompson, J.R., Bartlett, S.E., Ngo, S.T., Hilliard, M.A., Bellingham, M.C., Noakes, P.G., 2016. Cortical synaptic and dendritic spine abnormalities in a presymptomatic TDP-43 model of amyotrophic lateral sclerosis. Sci Rep 6:37968. http://dx.doi.org/10.1038/srep37968.

Foran, E., Trotti, D., 2009. Glutamate transporters and the excitotoxic path to motor neuron degeneration in amyotrophic lateral sclerosis. Antioxid. Redox Signal. 11: 1587–1602. http://dx.doi.org/10.1089/ars.2009.2444.

Frantseva, M.V., Perez Velazquez, J.L., Carlen, P.L., 1998. Changes in membrane and synaptic properties of thalamocortical circuitry caused by hydrogen peroxide. J. Neurophysiol. 80, 1317–1326.

Geevasinga, N., Menon, P., Yiannikas, C., Kiernan, M.C., Vucic, S., 2014. Diagnostic utility of cortical excitability studies in amyotrophic lateral sclerosis. Eur. J. Neurol. 21: 1451–1457. http://dx.doi.org/10.1111/ene.12422.

Gogvadze, V.G., Zhukova, A.A., 1991. The role of lipid peroxidation products in cumene hydroperoxide-induced Ca^{2+} efflux from mitochondria. FEBS Lett. 287 (1–2), 139–141.

Grosskreutz, J., Haastert, K., Dewil, M., Van Damme, P., Callewaert, G., Robberecht, W., Dengler, R., Van Den Bosch, L., 2007. Role of mitochondria in kainate-induced fast Ca^{2+} transients in cultured spinal motor neurons. Cell Calcium 42:59–69. http://dx.doi.org/10.1016/j.ceca.2006.11.010.

Guatteo, E., Carunchio, I., Pieri, M., Albo, F., Canu, N., Mercuri, N.B., Zona, C., 2007. Altered calcium homeostasis in motor neurons following AMPA receptor but not voltage-dependent calcium channels' activation in a genetic model of amyotrophic lateral sclerosis. Neurobiol. Dis. 28:90–100. http://dx.doi.org/10.1016/j.nbd.2007.07.002.

Han, J., Ma, L., 2010. Study of the features of proton MR spectroscopy ((1)H-MRS) on amyotrophic lateral sclerosis. J. Magn. Reson. Imaging 31:305–308. http://dx.doi.org/10.1002/jmri.22053.

Heath, P.R., Shaw, P.J., 2002. Update on the glutamatergic neurotransmitter system and the role of excitotoxicity in amyotrophic lateral sclerosis. Muscle Nerve 26: 438–458. http://dx.doi.org/10.1002/mus.10186.

Ikawa, M., Okazawa, H., Tsujikawa, T., Matsunaga, A., Yamamura, O., Mori, T., Hamano, T., Kiyono, Y., Nakamoto, Y., Yoneda, M., 2015. Increased oxidative stress is related to disease severity in the ALS motor cortex: a PET study. Neurology 84:2033–2039. http://dx.doi.org/10.1212/WNL.0000000000001588.

Jovanovic, Z.D., Stanojevic, M.B., Nedeljkov, V.B., 2016. The neurotoxic effects of hydrogen peroxide and copper in Retzius nerve cells of the leech *Haemopis sanguisuga*. Biol. Open 5:381–388. http://dx.doi.org/10.1242/bio.014936.

Kim, C., Lee, H.C., Sung, J.-J., 2014. Amyotrophic lateral sclerosis – cell based therapy and novel therapeutic development. Exp. Neurobiol. 23:207–214. http://dx.doi.org/10.5607/en.2014.23.3.207.

King, A.E., Woodhouse, A., Kirkcaldie, M.T.K., Vickers, J.C., 2016. Excitotoxicity in ALS: overstimulation, or overreaction? Exp. Neurol. 275:162–171. http://dx.doi.org/10.1016/j.expneurol.2015.09.019.

Kuo, J.J., Siddique, T., Fu, R., Heckman, C.J., 2005. Increased persistent Na(+) current and its effect on excitability in motoneurones cultured from mutant SOD1 mice. J. Physiol. 563:843–854. http://dx.doi.org/10.1113/jphysiol.2004.074138.

Kwak, S., Hideyama, T., Yamashita, T., Aizawa, H., 2010. AMPA receptor-mediated neuronal death in sporadic ALS. Neuropathology 30:182–188. http://dx.doi.org/10.1111/j.1440-1789.2009.01090.x.

Lloyd, C.M., Richardson, M.P., Brooks, D.J., Al-Chalabi, A., Leigh, P.N., 2000. Extramotor involvement in ALS: PET studies with the GABA(A) ligand [(11)C]flumazenil. Brain 2289–2296.

Maekawa, S., Al-Sarraj, S., Kibble, M., Landau, S., Parnavelas, J., Cotter, D., Everall, I., Leigh, P.N., 2004. Cortical selective vulnerability in motor neuron disease: a morphometric study. Brain 127:1237–1251. http://dx.doi.org/10.1093/brain/awh132.

Malessa, S., Leigh, P.N., Bertel, O., Sluga, E., Hornykiewicz, O., 1991. Amyotrophic lateral sclerosis: glutamate dehydrogenase and transmitter amino acids in the spinal cord. J. Neurol. Neurosurg. Psychiatry 54, 984–988.

Martin, L.J., Chang, Q., 2012. Inhibitory synaptic regulation of motoneurons: a new target of disease mechanisms in amyotrophic lateral sclerosis. Mol. Neurobiol. 45:30–42. http://dx.doi.org/10.1007/s12035-011-8217-x.

Martorana, F., Brambilla, L., Valori, C.F., Bergamaschi, C., Roncoroni, C., Aronica, E., Volterra, A., Bezzi, P., Rossi, D., 2012. The BH4 domain of Bcl-XL rescues astrocyte degeneration in amyotrophic lateral sclerosis by modulating intracellular calcium signals. Hum. Mol. Genet. 21:826–840. http://dx.doi.org/10.1093/hmg/ddr513.

McGown, A., McDearmid, J.R., Panagiotaki, N., Tong, H., Al Mashhadi, S., Redhead, N., Lyon, A.N., Beattie, C.E., Shaw, P.J., Ramesh, T.M., 2013. Early interneuron dysfunction in ALS: insights from a mutant sod1 zebrafish model. Ann. Neurol. 73:246–258. http://dx.doi.org/10.1002/ana.23780.

Mochizuki, Y., Mizutani, T., Shimizu, T., Kawata, A., 2011. Proportional neuronal loss between the primary motor and sensory cortex in amyotrophic lateral sclerosis. Neurosci. Lett. 503:73–75. http://dx.doi.org/10.1016/j.neulet.2011.08.014.

Muñoz, M.F., Argüelles, S., Cano, M., Marotta, F., Ayala, A., 2017. Aging and oxidative stress decrease pineal elongation factor 2: in vivo protective effect of melatonin in young rats treated with cumene hydroperoxide. J. Cell. Biochem. 118:182–190. http://dx.doi.org/10.1002/jcb.25624.

Nakaya, H., Takeda, Y., Tohse, N., Kanno, M., 1992. Mechanism of the membrane depolarization induced by oxidative stress in guinea-pig ventricular cells. J. Mol. Cell. Cardiol. 24, 523–534.

Nam, T.-G., 2011. Lipid peroxidation and its toxicological implications. Toxicol. Res. 27: 1–6. http://dx.doi.org/10.5487/TR.2011.27.1.001.

Nani, F., Cifra, A., Nistri, A., 2010. Transient oxidative stress evokes early changes in the functional properties of neonatal rat hypoglossal motoneurons *in vitro*. Eur. J. Neurosci. 31:951–966. http://dx.doi.org/10.1111/j.1460-9568.2010.07108.x.

Niebroj-Dobosz, I., Janik, P., 1999. Amino acids acting as transmitters in amyotrophic lateral sclerosis (ALS). Acta Neurol. Scand. 100, 6–11.

Niedzielska, E., Smaga, I., Gawlik, M., Moniczewski, A., Stankowicz, P., Pera, J., Filip, M., 2016. Oxidative stress in neurodegenerative diseases. Mol. Neurobiol. 53: 4094–4125. http://dx.doi.org/10.1007/s12035-015-9337-5.

Nieto-Gonzalez, J.L., Moser, J., Lauritzen, M., Schmitt-John, T., Jensen, K., 2011. Reduced GABAergic inhibition explains cortical hyperexcitability in the wobbler mouse model of ALS. Cereb. Cortex 21:625–635. http://dx.doi.org/10.1093/cercor/bhq134.

Nihei, K., Kowall, N.W., 1993. Involvement of NPY-immunoreactive neurons in the cerebral cortex of amyotrophic lateral sclerosis patients. Neurosci. Lett. 159, 67–70.

Pardillo-Díaz, R., Carrascal, L., Ayala, A., Nunez-Abades, P., 2015. Oxidative stress induced by cumene hydroperoxide evokes changes in neuronal excitability of rat motor cortex neurons. Neuroscience 289C:85–98. http://dx.doi.org/10.1016/j.neuroscience.2014.12.055.

Pardillo-Díaz, R., Carrascal, L., Muñoz, M.F., Ayala, A., Nunez-Abades, P., 2016. Time and dose dependent effects of oxidative stress induced by cumene hydroperoxide in neuronal excitability of rat motor cortex neurons. Neurotoxicology:53. http://dx.doi.org/10.1016/j.neuro.2016.02.005.

Petri, S., Krampfl, K., Hashemi, F., Grothe, C., Hori, A., Dengler, R., Bufler, J., 2003. Distribution of GABAA receptor mRNA in the motor cortex of ALS patients. J. Neuropathol. Exp. Neurol. 62, 1041–1051.

Philips, T., Robberecht, W., 2011. Neuroinflammation in amyotrophic lateral sclerosis: role of glial activation in motor neuron disease. Lancet Neurol. 10:253–263. http://dx.doi.org/10.1016/S1474-4422(11)70015-1.

Pieri, M., Carunchio, I., Curcio, L., Mercuri, N.B., Zona, C., 2009. Increased persistent sodium current determines cortical hyperexcitability in a genetic model of amyotrophic lateral sclerosis. Exp. Neurol. 215:368–379. http://dx.doi.org/10.1016/j.expneurol.2008.11.002.

Pieri, M., Caioli, S., Canu, N., Mercuri, N.B., Guatteo, E., Zona, C., 2013. Over-expression of N-type calcium channels in cortical neurons from a mouse model of Amyotrophic Lateral Sclerosis. Exp. Neurol. 247:349–358. http://dx.doi.org/10.1016/j.expneurol.2012.11.002.

Pioro, E.P., Majors, A.W., Mitsumoto, H., Nelson, D.R., Ng, T.C., 1999. 1H-MRS evidence of neurodegeneration and excess glutamate + glutamine in ALS medulla. Neurology 53, 71–79.

Poppe, L., Rué, L., Robberecht, W., Van Den Bosch, L., 2014. Translating biological findings into new treatment strategies for amyotrophic lateral sclerosis (ALS). Exp. Neurol. 262 (Pt B):138–151. http://dx.doi.org/10.1016/j.expneurol.2014.07.001.

Reynolds, A., Laurie, C., Lee Mosley, R., Gendelman, H.E., 2007. Oxidative stress and the pathogenesis of neurodegenerative disorders. International Review of Neurobiology:pp. 297–325. http://dx.doi.org/10.1016/S0074-7742(07)82016-2.

Saba, L., Viscomi, M.T., Caioli, S., Pignataro, A., Bisicchia, E., Pieri, M., Molinari, M., Ammassari-Teule, M., Zona, C., 2016. Altered functionality, morphology, and vesicular glutamate transporter expression of cortical motor neurons from a presymptomatic mouse model of amyotrophic lateral sclerosis. Cereb. Cortex 26:1512–1528. http://dx.doi.org/10.1093/cercor/bhu317.

Sasabe, J., Aiso, S., 2010. Aberrant control of motoneuronal excitability in amyotrophic lateral sclerosis: excitatory glutamate/D-serine vs. inhibitory glycine/γ-aminobutanoic acid (GABA). Chem. Biodivers. 7:1479–1490. http://dx.doi.org/10.1002/cbdv.200900306.

Sebe, J.Y., Looke-Stewart, E.C., Estrada, R.C., Baraban, S.C., 2010. Robust tonic GABA currents can inhibit cell firing in mouse newborn neocortical pyramidal cells. Eur. J. Neurosci. 32:1310–1318. http://dx.doi.org/10.1111/j.1460-9568.2010.07373.x.

Spalloni, A., Nutini, M., Longone, P., 2013. Role of the N-methyl-d-aspartate receptors complex in amyotrophic lateral sclerosis. Biochim. Biophys. Acta 1832:312–322. http://dx.doi.org/10.1016/j.bbadis.2012.11.013.

Takahashi, M., Kovalchuk, Y., Attwell, D., 1995. Pre- and postsynaptic determinants of EPSC waveform at cerebellar climbing fiber and parallel fiber to Purkinje cell synapses. J. Neurosci. 15, 5693–5702.

Torres-Torrelo, J., Rodriguez-Rosell, D., Nunez-Abades, P., Carrascal, L., Torres, B., 2012. Glutamate modulates the firing rate in oculomotor nucleus motoneurons as a function of the recruitment threshold current. J. Physiol. 590:3113–3127. http://dx.doi.org/10.1113/jphysiol.2011.226985.

Torres-Torrelo, J., Torres, B., Carrascal, L., 2014. Modulation of the input-output function by GABAA receptor-mediated currents in rat oculomotor nucleus motoneurons. J. Physiol. 592:5047–5064. http://dx.doi.org/10.1113/jphysiol.2014.276576.

Turner, M.R., Kiernan, M.C., 2012. Does interneuronal dysfunction contribute to neurodegeneration in amyotrophic lateral sclerosis? Amyotroph. Lateral Scler. 13:245–250. http://dx.doi.org/10.3109/17482968.2011.636050.

Turner, M.R., Kiernan, M.C., Leigh, P.N., Talbot, K., 2009. Biomarkers in amyotrophic lateral sclerosis. Lancet Neurol. 8:94–109. http://dx.doi.org/10.1016/S1474-4422(08)70293-X.

Van Den Bosch, L., Van Damme, P., Bogaert, E., Robberecht, W., 2006. The role of excitotoxicity in the pathogenesis of amyotrophic lateral sclerosis. Biochim. Biophys. Acta - Mol. Basis Dis. 1762:1068–1082. http://dx.doi.org/10.1016/j.bbadis.2006.05.002.

Vimard, F., Saucet, M., Nicole, O., Feuilloley, M., Duval, D., 2011. Toxicity induced by cumene hydroperoxide in PC12 cells: protective role of thiol donors. J. Biochem. Mol. Toxicol. 25:205–215. http://dx.doi.org/10.1002/jbt.20377.

Vucic, S., Nicholson, G.A., Kiernan, M.C., 2008. Cortical hyperexcitability may precede the onset of familial amyotrophic lateral sclerosis. Brain 131:1540–1550. http://dx.doi.org/10.1093/brain/awn071.

Vucic, S., Cheah, B.C., Yiannikas, C., Kiernan, M.C., 2011. Cortical excitability distinguishes ALS from mimic disorders. Clin. Neurophysiol. 122:1860–1866. http://dx.doi.org/10.1016/j.clinph.2010.12.062.

Wagle-Shukla, A., Ni, Z., Gunraj, C.A., Bahl, N., Chen, R., 2009. Effects of short interval intracortical inhibition and intracortical facilitation on short interval intracortical facilitation in human primary motor cortex. J. Physiol. 587:5665–5678. http://dx.doi.org/10.1113/jphysiol.2009.181446.

Yin, B., Barrionuevo, G., Batinic-Haberle, I., Sandberg, M., Weber, S.G., 2017. Differences in Reperfusion-induced Mitochondrial Oxidative Stress and Cell Death Between Hippocampal CA1 And CA3 Subfields is Due to the Mitochondrial Thioredoxin System. Antioxid Redox Signal. 2017 Jan 27. http://dx.doi.org/10.1089/ars.2016.6706.

Zanette, G., Tamburin, S., Manganotti, P., Refatti, N., Forgione, A., Rizzuto, N., 2002. Different mechanisms contribute to motor cortex hyperexcitability in amyotrophic lateral sclerosis. Clin. Neurophysiol. 113, 1688–1697.

Zhang, W., Zhang, L., Liang, B., Schroeder, D., Zhang, Z., Cox, G.A., Li, Y., Lin, D.-T., 2016. Hyperactive somatostatin interneurons contribute to excitotoxicity in neurodegenerative disorders. Nat. Neurosci. 19:557–559. http://dx.doi.org/10.1038/nn.4257.

Ziemann, U., Winter, M., Reimers, C.D., Reimers, K., Tergau, F., Paulus, W., 1997. Impaired motor cortex inhibition in patients with amyotrophic lateral sclerosis. Evidence from paired transcranial magnetic stimulation. Neurology 49, 1292–1298.

Zoccolella, S., Santamato, A., Lamberti, P., 2009. Current and emerging treatments for amyotrophic lateral sclerosis. Neuropsychiatr. Dis. Treat. 5, 577–595.

Zona, C., Pieri, M., Carunchio, I., 2006. Voltage-dependent sodium channels in spinal cord motor neurons display rapid recovery from fast inactivation in a mouse model of amyotrophic lateral sclerosis. J. Neurophysiol. 96:3314–3322. http://dx.doi.org/10.1152/jn.00566.2006.